

# Evidence for a Functional Link between Uncoating of the Human Immunodeficiency Virus Type 1 Core and Nuclear Import of the Viral Preintegration Complex

David J. Dismuke and Christopher Aiken\*

*Department of Microbiology and Immunology, Vanderbilt University School of Medicine, Nashville, Tennessee 37232*

Received 1 August 2005/Accepted 31 January 2006

**Human immunodeficiency virus type 1 (HIV-1) particles begin their replication upon fusion with the plasma membrane of target cells and release of the viral core into the host cell cytoplasm. Soon thereafter, the viral capsid, which is composed of a polymer of the CA protein, disassociates from the internal ribonucleoprotein complex. While this disassembly process remains poorly understood, the available evidence indicates that proper uncoating of the core is a key step in infection. Defects in uncoating most often lead to a failure of the virus to undergo reverse transcription, resulting in an inability to form a functional viral preintegration complex (PIC). In a previous study, we reported that an HIV-1 mutant containing two substitutions in CA (Q63A/67A) was unusual in that it was poorly infectious yet synthesized normal levels of viral DNA. Here we report that this mutant is impaired for nuclear entry. Quantitative analysis of viral DNA synthesis from infected cells by Southern blotting and real-time PCR revealed that the Q63A/Q67A mutant is impaired in the synthesis of one-long terminal repeat (1-LTR) and 2-LTR circles. Isolation of PICs from acutely infected cells revealed that the Q63A/Q67A mutant produces protein-DNA complexes similar to wild-type in yield and overall composition, but these PICs contained elevated levels of CA and were impaired for integration *in vitro*. These results demonstrate that mutations in CA can have deleterious effects on both nuclear targeting and integration, suggesting that these steps in the HIV-1 life cycle are dependent on proper uncoating of the viral core.**

Primate lentiviruses are characterized by two predominant features: the presence of a conical core and the ability to infect nondividing cells. The core of human immunodeficiency virus type 1 (HIV-1) is composed of a ribonucleoprotein complex (RNP) surrounded by a capsid shell, which consists of a polymer of the CA protein. For productive infection, the RNA within this complex must be converted to double-stranded DNA and enter the nucleus to subsequently integrate into the host genome. While much is known about the structure of the viral capsid, the precise role that CA plays in postentry events remains poorly defined.

Formation of the conical viral capsid occurs during the process of viral maturation. During particle release, the viral protease (PR) is activated and cleaves the 55-kDa Gag polypeptide into the structural proteins MA, CA, and NC and p6. Cleavage of Gag is a temporally ordered process, with release of CA representing the terminal step. During maturation, the virus undergoes dramatic morphological changes in which NC coats the RNA genome, MA associates with the viral lipid envelope, and approximately 1,500 molecules of CA condense to form the mature viral capsid (5).

Upon fusion of viral and host cell membranes and concomitant release of the viral core into the cytoplasm, the core subsequently uncoats. In this process the viral capsid disassembles, releasing the viral RNP. HIV-1 uncoating has generally been assumed to occur shortly after fusion, as electron-microscopic analysis of HIV-1-infected cells has failed to detect the

presence of lentiviral cores in the cytoplasm (27). However, previous work from our laboratory has demonstrated that HIV-1 uncoating is a finely tuned process, with mutations in CA that alter the capsid stability resulting in impaired HIV-1 infectivity (25). The majority of such mutants exhibited a postentry impairment in reverse transcription. By contrast, two HIV-1 mutants that exhibited reduced capsid stability (P38A and Q63A/Q67A) were competent for DNA synthesis, suggesting an involvement of CA in nuclear import and/or integration.

Following uncoating and reverse transcription, HIV-1 DNA is present in the cytoplasm in a high-molecular-weight nucleoprotein complex termed the preintegration complex (PIC). The viral proteins present in this complex are integrase (IN), MA, reverse transcriptase (RT), NC, and Vpr (9, 19, 21, 36). HIV-1 PICs contain little to no CA (9, 19, 21, 36). Several cellular proteins have also been described as specifically interacting with the PIC, presumably increasing the proper integration of the provirus (18, 30). Although the structure of the PIC is not known, studies have suggested that the ends of the DNA are tethered by an assemblage of proteins that likely serve to protect and prime the ends for integration (16, 28, 36). IN, in particular, is an important component of this complex and catalyzes the terminal cleavage and ligation reactions necessary for integration.

By contrast to simple retroviruses, lentiviruses such as HIV-1 are capable of infecting nonmitotic cells, suggesting that they have a mechanism for active transport into the nucleus. Nuclear import of the HIV-1 PIC is an ATP-dependent process (8), which suggests the involvement of the nuclear transport pathway and a viral nuclear localization signal. Of the virus-associated proteins, IN, MA, and Vpr have all been reported to have karyophilic properties (4, 7, 38). A proviral

\* Corresponding author. Mailing address: Department of Microbiology and Immunology, Vanderbilt University School of Medicine, A-5301 Medical Center North, Nashville, TN 37232-2363. Phone: (615) 343-7037. Fax: (615) 343-7392. E-mail: chris.aiken@vanderbilt.edu.

structure known as the central DNA flap may also be important for nuclear targeting (2, 17, 29, 47). Despite these observations, at present no clear consensus on the viral determinants of HIV-1 nuclear import exists. Interestingly, a recent study using HIV-1/murine leukemia virus (MLV) chimeric viruses indicated that the HIV-1 CA protein is a key determinant for infection of nonmitotic cells (44), suggesting a possible link between uncoating and nuclear import of the PIC.

In this study we have analyzed in detail the phenotype of a poorly infectious HIV-1 mutant, Q63/67A, which encodes two Gln-to-Ala substitutions in CA. This mutant has an unusual phenotype in that it produces unstable cores yet is competent for reverse transcription in target cells. We show that the mutant PICs are defective for both nuclear targeting in cells and for integration *in vitro*; they also contain elevated levels of CA relative to wild-type PICs. Collectively, the results suggest that proper HIV-1 uncoating is required for subsequent postentry steps in the HIV-1 life cycle.

#### MATERIALS AND METHODS

**Cells and viruses.** 293T and HeLa-CD4/LTR-lacZ (P4) cells were cultured at 37°C in a 5% CO<sub>2</sub> humidified incubator in Dulbecco's modification of Eagle medium (Cellgro) supplemented with 10% fetal bovine serum (HyClone), penicillin (50 IU/ml), and streptomycin (50 µg/ml). SupT1 cells and Molt-IIIB cells were grown in RPMI 1640 (Cellgro) supplemented with 10% fetal bovine serum (HyClone), penicillin (50 IU/ml), and streptomycin (50 µg/ml) at 37°C and 5% CO<sub>2</sub>. HIV-1 proviral DNA constructs R9, containing full-length HIV-1, and R9 Env<sup>-</sup>, in which there is a frameshift mutation in the 5' end of the *env* gene (48), were the control viruses utilized in this study. HIV-1 proviral mutants encoding substitutions in CA were obtained from Wes Sundquist and were previously described (40). *env*-defective derivatives containing CA point mutations were generated by transferring BssHII-SpeI restriction fragments from R9 clones into the R9 Env<sup>-</sup> plasmid. All mutations were verified by sequencing. Viruses were produced by transient transfection of 293T cells using calcium phosphate (20 µg of plasmid DNA per 2 × 10<sup>6</sup> cells) as previously described (15). Pseudotyping of R9 Env<sup>-</sup> by the vesicular stomatitis virus glycoprotein (VSV-G) was performed by cotransfection with pHCMV-G (2 µg) (46). Two days after transfection virus-containing supernatant was collected and clarified by filtration through 0.45-µm-pore-size filters and frozen in aliquots at -80°C. The CA content of the virus stocks was quantified by a p24-specific enzyme-linked immunosorbent assay (ELISA) utilizing monoclonal antibody 183 for capture (42).

**HIV-1 infection assays.** The multinucleate activation of galactosidase indicator cell assay was used to measure virus infectivity on HeLa-CD4/LTR-lacZ (P4) cells as previously described (13). One day prior to infection, P4 indicator cells were plated in 48-well plates (2 × 10<sup>4</sup> cells per well). Viral inocula were normalized for p24 content and supplemented with DEAE-dextran (20 µg/ml). Cultures were fixed and stained with 5-bromo-4-chloro-3-indolyl-β-D-galactopyranoside (X-Gal) 48 h postinfection, and infected cells were counted using NIH Image software. Infectivity values were reported as the number of blue foci per ng of p24 antigen. For determining infectivity of virus on SupT1 cells, intracellular p24 was quantified by flow cytometry. Cells were fixed and permeabilized with Cytoperm/Cytofix reagents (BD Pharmingen) 48 h postinfection, and intracellular p24 was detected by staining with CA-specific mouse monoclonal antibody 183 (NIH AIDS Research and Reference Reagent Program) followed by allophycocyanin-labeled goat anti-mouse secondary antibody (BD Pharmingen). Flow cytometry was performed using a Becton Dickinson FACScalibur and the percentage of green fluorescent protein- or p24-expressing cells quantified using Cellquest software. A minimum of 10,000 cells were analyzed for each sample.

**Virus-cell fusion assay.** The BlaM-Vpr HIV-1 fusion assays were performed essentially as previously described (43). Quantities of wild-type and mutant reporter viruses were normalized by p24 content and used to inoculate SupT1 target cells for 2 h at 37°C. Cells were then loaded with the CCF2-AM fluorogenic substrate overnight at room temperature. Cells were then centrifuged and the supernatant replaced with phosphate-buffered saline (PBS). Cellular fluorescence was determined in a microplate fluorometer. The background levels of blue (no virus) and green fluorescence (no cells or virus) were determined at 410 nm and 520 nm, respectively, and were subtracted from the experimental

samples. Fluorescence ratios were calculated for each well. For each virus dilution, triplicate determinations were performed, and values typically agreed to within 10%.

**Quantitative analysis of HIV-1 reverse transcription in target cells.** One day prior to infection 200,000 P4 or SupT1 target cells were plated per well in 12-well plates. Viruses were treated with 20 µg/ml of DNase I and 10 mM MgCl<sub>2</sub> at 37°C for 1 hour to remove contaminating plasmid DNA. Inocula were normalized by p24 content to 100 ng per well for viruses bearing HIV-1 envelope or 10 ng/well for viruses possessing VSV-G in medium containing DEAE-dextran at 10 µg/ml. At various times postinfection, infected cells were washed with 1 ml of PBS and then treated with 500 µl of trypsin. Trypsin was deactivated by addition of 750 µl of Dulbecco's modification of Eagle medium containing 10% fetal bovine serum, and cells were collected and washed once with 500 µl of PBS. Cell pellets were resuspended in 200 µl of PBS, and DNA was isolated using a DNeasy kit (QIAGEN) by following manufacturer's instructions. Viral DNA was quantified by real-time PCR using an MX-3000p thermocycler (Stratagene) utilizing TaqMan chemistry (ABI). Early reverse transcription products (minus-strand strong-stop DNA) were detected using forward primer ERT-SS-F (5'-GCTAACTAG GGAACCCACTGCTT-3'), reverse primer ERT-SS-R (5'-ACAACAGACGGG CACACTAC-3'), and early product probe ERT-SS-Probe (5'-[6-carboxyfluorescein {FAM}]-AGCCTCAATAAAGCTTGCCCTGAGTGCTTC-[6-carboxy tetramethylrhodamine {TAMRA}]-3'). Late reverse transcription products (U5-Gag) were detected using the forward primer MH531 (5'-TGTTGTCGCCGTCTGTGT GT-3') and reverse primer MH532 (5'-GAGTCTGCGTCGAGAGAGC-3'), with the probe LRT-P (5'-[FAM]-CAGTGGCGCCGAACAGGGA-[TAMRA]-3') as previously described (10). Thermal cycling conditions were 2 min at 50°C, 10 min at 95°C, and 40 cycles of 95°C for 15 seconds and 60°C for 60 seconds.

**Quantitative analysis of HIV-1 *in vivo* integration in target cells.** For analysis of *in vivo* integration, VSV-G-pseudotyped viruses were treated with 20 µg/ml of DNase I and 10 mM MgCl<sub>2</sub> at 37°C for 1 hour to remove contaminating plasmid DNA. Cell-free viruses were normalized by p24 content to 100 ng and used to infect 1 × 10<sup>5</sup> SupT1 target cells. Cells were cultured for 14 days to allow degradation of nonintegrated viral DNA. DNA was isolated from cells by DNeasy kit (QIAGEN) and was subjected to nested quantitative PCR as previously described (6). Twofold serial dilutions of DNA from cells infected with wild-type virus were used to generate a standard curve. Integrated proviral DNA was detected using first-round primers specific for the HIV long terminal repeat (LTR) and human genomic Alu elements. The forward primer L-M667 (5'-A TGCCACGTAAGCGAACTCTGGCTAACTAGGGAACCCACTG-3') and the reverse primers Alu 1 (5'-TCCCAGTACTGGGGAGGCTGAGG-3') and Alu 2 (5'-GCCTCCCAAAGTGTGGGATTACAG-3') were used for the first round of PCR. Conditions for the initial round of amplification were 10 min at 95°C, followed by 12 cycles of 95°C for 10 s, 60°C for 10 s, and 72°C for 120 s. One-tenth volume of the first round of PCR was subjected to a second round of quantitative PCR. For the detection round of real-time PCR, the forward primer Lambda T (5'-ATGCCACGTAAGCGAACT-3'), the reverse primer AA55M (5'-GCTAGAGATTTCCCACTGACTAA-3'), and 2-LTR probe TaqMan MH603 were used. Second-round amplification conditions were 10 min at 95°C and 40 cycles of 95°C for 10 s, 60°C for 10 s, and 72°C for 9 s.

**Isolation and analysis of PICs.** VSV-G-pseudotyped viruses were treated with 20 µg/ml of DNase I and 10 mM MgCl<sub>2</sub> at 37°C for 1 hour to remove contaminating plasmid DNA. Cell-free viruses were normalized by p24 content to 150 µg and used to infect 5 × 10<sup>8</sup> SupT1 target cells. Cytoplasmic extracts were prepared from infected cells 8 h after infection as previously described (20). Briefly, cells were washed with cold buffer K (20 mM HEPES, pH 7.4, 5 mM MgCl<sub>2</sub>, 150 mM KCl, 1 mM dithiothreitol, and 10 kallikrein inhibitor units/ml aprotinin) and treated with 15 ml buffer K containing 0.05% Triton X-100 (Pierce) for 10 min at room temperature. Cells were pelleted by centrifugation for 3 min at 1,000 × g, and then the supernatant was clarified by centrifugation for 3 min at 8,000 × g. Aliquots of cytoplasmic extracts were snap-frozen in liquid nitrogen and stored at -80°C.

*In vitro* integration reactions were performed by incubating 200 µl of the PIC extracts with 1 µg of double-stranded replicative form of φX174 DNA (New England Biolabs) for 45 min at 37°C. As a control, L-839616 (Merck), referred to as compound 5 (41), a potent and specific inhibitor of integration, was added in some reactions to a final concentration of 1 µM. After integration, the DNA from the reactions was collected by DNeasy kit isolation (QIAGEN) and integration was quantified using a novel real-time PCR-based approach, the details of which will be reported elsewhere. Briefly, reaction mixtures contained six primers specific for one strand of the double-stranded replicative form of φX174 DNA. The MH535 primer (5'-AACTAGGGAACCCACTGCTTAAAG-3') and MH603 probe (5'-[FAM]-ACACTACTTGAAGCACTCAAGGCAAGCTTT-[TAMRA]-3') were utilized to recognize the HIV-1 LTR. Integration reactions

containing twofold serial dilutions of wild-type cytoplasmic extracts were used to generate a relative standard curve for demonstrating the dose dependence of the integration signal.

**Velocity gradient analysis and immunoblotting of PICs.** To partially purify PICs for biochemical analysis, PIC-containing extracts (1 ml) were loaded onto 10 to 50% linear sucrose gradients and centrifuged at 32,000 rpm ( $137,000 \times g$ ) in an SW-32.1Ti Beckman rotor at 4°C for 2 h. Fractions (1 ml) were collected, and viral late reverse transcripts were quantified from DNA isolated from 100  $\mu$ l of each fraction. Exogenous reverse transcriptase activity assays were performed using 10  $\mu$ l from each fraction as previously described (25). For immunoblotting, proteins present in 200  $\mu$ l of each fraction were concentrated by trichloroacetic acid precipitation and subjected to electrophoresis on 4 to 20% gradient polyacrylamide denaturing gels (Bio-Rad). Proteins were transferred electrophoretically to Protran nitrocellulose membranes (Perkin-Elmer) and probed with monoclonal mouse or polyclonal rabbit antibodies specific for viral proteins, including mouse anti-MA, mouse anti-CA (183), and rabbit anti-IN. Primary antibodies were probed using goat anti-mouse-Alexa 680 and goat anti-rabbit-Alexa 800. Protein detection and quantitation were performed with an Odyssey infrared imaging station (Li-Cor).

**Assays of HIV-1 nuclear targeting.** DNA from acutely infected cells was isolated at various times postinfection by phenol-chloroform extraction or using the DNeasy kit (QIAGEN) and analyzed for the presence of 1-LTR or 2-LTR circles, respectively. For detection of 1-LTR circles, 10  $\mu$ g of total DNA was digested with MscI and XhoI, transferred onto nitrocellulose membranes by Southern blotting, and analyzed using a  $^{32}$ P-labeled probe overlapping the 5' MscI site as previously described (47). 2-LTR circle DNA was detected by quantitative real-time PCR utilizing primers and a TaqMan probe specific for the LTR-LTR junction. The forward primer MH535 (5'-AACTAGGGAACCCAC TGCTTAAG-3'), the reverse primer MH536 (5'-TCCACAGATCAAGGATA TCTTGTC-3'), and 2-LTR probe MH603 (5'-[FAM]-ACACTACTGAAGCA CTCAAGGCAAGCTTT-[TAMRA]-3') were used. Thermal cycling conditions were 2 min at 50°C, 10 min at 95°C, and 40 cycles of 95°C for 15 seconds and 60°C for 60 seconds.

## RESULTS

**CA mutants are impaired for infection at a step following fusion.** Mutations within the CA region of HIV-1 can give rise to mutants blocked at early postentry or during assembly of progeny virions. Analysis of HIV-1 containing point mutations within CA has indicated that the double mutant Q63A/67A is capable of viral production and formation of conical cores but has altered core stability in vitro (25). Single-cycle infection analysis of this virus using HeLa-CD4/LTR-*lacZ* (P4) reporter cells demonstrated that it is poorly infectious relative to wild-type virus (Fig. 1A). As a control for these studies, we included the noninfectious CA mutant K203A, which contains unstable cores and is impaired for reverse transcription in target cells (25). Since a positive signal in this assay requires only that the incoming virus integrate and express the Tat protein, the poor infectivity suggests that the Q63/67A CA mutant is impaired for an early postentry step in the virus life cycle. To determine whether fusion was affected, we assayed this directly using a recently described virus-cell reporter fusion assay (12). Wild-type and mutant viruses containing BlaM-Vpr were produced by cotransfection of 293T cells with HIV-1 proviral clones and a BlaM-Vpr expression plasmid. The particles were then titrated onto SupT1 target cells. Wild-type and Q63/67A particles exhibited similar levels of fusion across a range of virus dilutions (Fig. 1B). Single-cycle infectivity assays using SupT1 cells as targets confirmed that the Q63/67A mutant was also poorly infectious in these cells (data not shown). These results suggested that the Q63/67A substitutions in CA do not impair the virus for entry into target cells but inhibit steps occurring between fusion and integration.

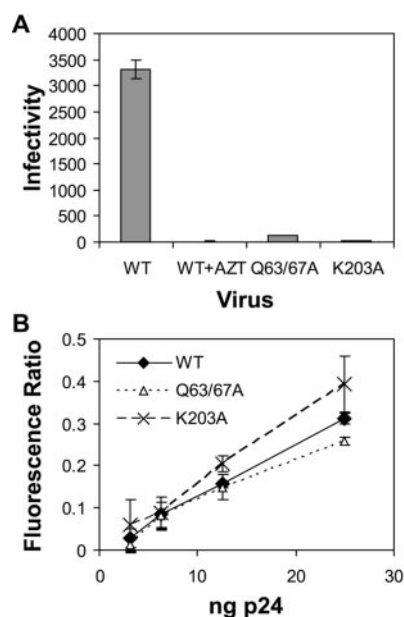


FIG. 1. Q63/67A particles are poorly infectious but are competent for cell entry. (A) Wild type (WT) and CA mutant (Q63/67A and K203A) viruses were used to infect CD4-expressing HeLa reporter cells (P4) in a single cycle. Virus input quantities were normalized by p24 ELISA. Infected cells were identified by staining with X-Gal. Shown are the mean values for triplicate infections, with error bars representing one standard deviation. Results are representative of seven independent experiments. (B) SupT1 cells were inoculated with wild-type and CA mutant viruses containing BlaM-Vpr and were subsequently loaded with CCF2-AM substrate. Fusion was quantified by determining the extent of substrate conversion resulting from release of BlaM in the target cytoplasm and was determined by measuring the ratio of blue to green fluorescence. Each virus dilution was analyzed in triplicate. Shown are the mean values, with error bars representing one standard deviation. Results are representative of seven independent experiments.

**Q63/67A virions are competent for reverse transcription in target cells.** In a previous study, we reported that the HIV-1 CA mutant Q63/67A was unusual: despite the reduced stability we observed for the mutant cores, the particles were competent for reverse transcription in target cells. To explore the kinetics of reverse transcription for this virus in greater detail, we quantified early and late reverse transcripts synthesized during a 25-h time course. Wild-type and mutant viruses were used to infect P4 target cells. At various times postinfection, infected cells were harvested and the DNA was purified. Quantitative real-time PCR was performed using primers and TaqMan probes specific for minus-strand strong-stop DNA. The mutant virus produced levels of early RT products similar to wild type, and at similar rates (Fig. 2A). At the 25-h time point, the levels of Q63/67A viral DNA had declined markedly, while the wild-type cDNA levels remained high, likely due to second-round infection by this replication-competent virus. By contrast, the poorly infectious CA mutant K203A synthesized low levels of early reverse transcripts at all time points tested, as did the wild-type virus inoculated in cells to which the reverse transcriptase inhibitor zidovudine (AZT) was added. We also quantified the late products of reverse transcription by analysis of samples using primers and a probe specific for full-length plus-strand DNA. The capacity of Q63/67A to synthesize late

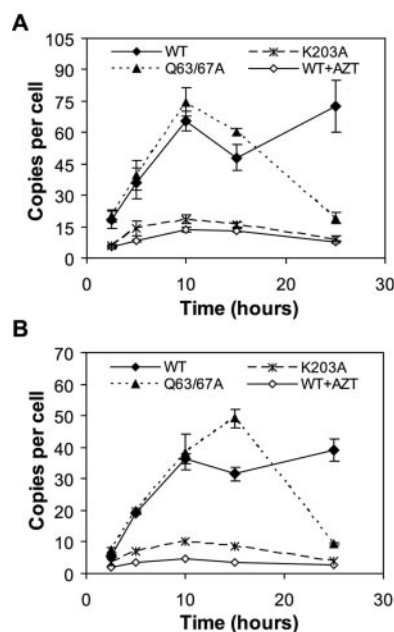


FIG. 2. Entry of Q63/67A mutant particles results in synthesis of normal levels of reverse transcripts. Wild-type (WT), Q63/67A, and K203A viruses were used to infect P4 cells in duplicate infections. At various times postinfection the DNA from target cells was isolated and HIV-1 early (A) and late (B) reverse transcripts were quantified by TaqMan real-time PCR for each sample in duplicate. Standards were generated by serial dilution of provirus containing plasmid DNA. For the AZT-treated control sample, cells were pretreated with drug 4 h prior to inoculation with wild-type HIV-1. The results represent the average of four determinations (duplicate measurements from two parallel samples), with error bars representing one standard deviation. Results are representative of six independent experiments.

reverse transcripts was normal (Fig. 2B). The ability of Q63/67A to generate wild-type quantities of late reverse transcription products indicates that the reduced infectivity of this mutant is likely due to a step in the life cycle following reverse transcription, such as nuclear import or integration.

**Pseudotyping of Q63/67A by VSV-G does not rescue its infectivity defect.** Pseudotyping HIV-1 with envelope proteins of other viruses enables some HIV-1 mutants to bypass early postentry blocks. Examples include HIV-1 MA and Nef mutants and virions produced in the presence of cyclosporine (1, 14, 26, 32, 34). Pseudotyping with some viral envelopes, such as VSV-G, alters the pathway of virus entry, targeting fusion to a low-pH endosomal compartment (1, 32). To determine if the block to infection for the Q63/67A mutant is dependent upon its route of entry in target cells, we performed single-cycle infections with wild-type and CA mutant HIV-1 particles that had been pseudotyped by VSV-G. Pseudotyped particles were titrated on P4, SupT1, and 293T cells. Cells were harvested 3 days after infection, and infected cells were identified by X-Gal staining for  $\beta$ -galactosidase activity (P4 cells) and by antibody staining for intracellular Gag expression followed by flow cytometry (SupT1 and 293T cells). VSV-G pseudotyping markedly enhanced the infectivity of wild-type and CA mutant viruses ( $\sim 10$ -fold; Fig. 3A), consistent with previous reports (1, 3, 32). Pseudotyping of CA mutants failed to restore normal infectivity in P4 cells (Fig. 3A) or in SupT1 and 293T cells (Fig.

3B and C). To confirm that the block to infection by the pseudotyped CA mutant virions was also at the level of reverse transcription, we quantified the synthesis of late reverse transcripts in P4 cells. As seen with nonpseudotyped virus, the VSV-pseudotyped Q63/67A and control viruses synthesized nearly equivalent levels of reverse transcription products in target cells (Fig. 3D). These results indicated that targeting HIV-1 entry to an endocytic route does not rescue the phenotype of the Q63/67A mutant particles. The conservation of the phenotype for Q63/67A particles pseudotyped with VSV-G also allowed us to use the pseudotyped viruses in studies of HIV-1 integration, as described below.

**Q63/67A is impaired for integration in target cells.** To determine whether the block for infectivity for Q63/67A occurs prior to integration, we analyzed the levels of integrated proviral DNA present in infected cells. For this purpose, VSV-pseudotyped viruses were used to enhance virus entry and prevent multiple rounds of infection that would otherwise occur with wild-type HIV-1. Pseudotyped particles were used to inoculate P4 cells, and infected cells were passaged for 14 days to allow the decay of unintegrated viral DNA. Cellular DNA was then isolated and subject to nested PCR to detect integrated proviral DNA. As expected, cells inoculated with the poorly infectious Q63/67A and K203A CA mutants exhibited low levels of integrated DNA (Fig. 4). Q63/67A displayed an approximately 10-fold reduction in integration. This reduction was apparently somewhat less than the loss of infectivity observed for this mutant, probably due to the background normally present in the nested-PCR-based assay for integrated viral DNA. The ability of the Q63/67A mutant to undergo reverse transcription but not integration prompted us to examine whether this mutant is competent for nuclear entry.

**Nuclear targeting of Q63/67A proviral DNA.** To test the ability of the mutant virus to target its DNA to the nucleus, we analyzed the presence of nuclear forms of viral DNA in target cells. Two markers for nuclear import of retroviral DNA are 1-LTR and 2-LTR circles. 1-LTR circles are formed by homologous recombination of the 5' and 3' LTRs, whereas 2-LTR circles are created by end-to-end ligation via the nonhomologous end-joining pathway (39). While these forms of viral DNA are unproductive products for the virus, they serve as useful and convenient reporters since they are found predominantly within the nuclei of infected cells. VSV-G-pseudotyped viruses were generated by transfection and used to infect SupT1 target cells. At various times postinfection the target cells were harvested and lysed, and DNA was isolated by phenol-chloroform extraction. We first quantified the levels of 2-LTR circles by quantitative PCR analysis of DNA from acutely infected cells. 2-LTR circles are found exclusively within the nuclei of infected cells and can be detected using primers that specifically amplify the LTR-LTR junction. Another advantage of this assay is the ability to determine the number of circles per cell by generating a standard curve with a plasmid containing a cloned LTR-LTR junction. Relative to wild-type HIV-1, cells inoculated with Q63/67A mutant particles were markedly deficient in 2-LTR circular DNA molecules (Fig. 5A). A lack of circular viral DNA strongly implies that the Q63/67A virus is impaired in its ability to access the nucleus.

A deficit in 2-LTR circle formation could also be due to a failure of the virus to synthesize the proper double-stranded

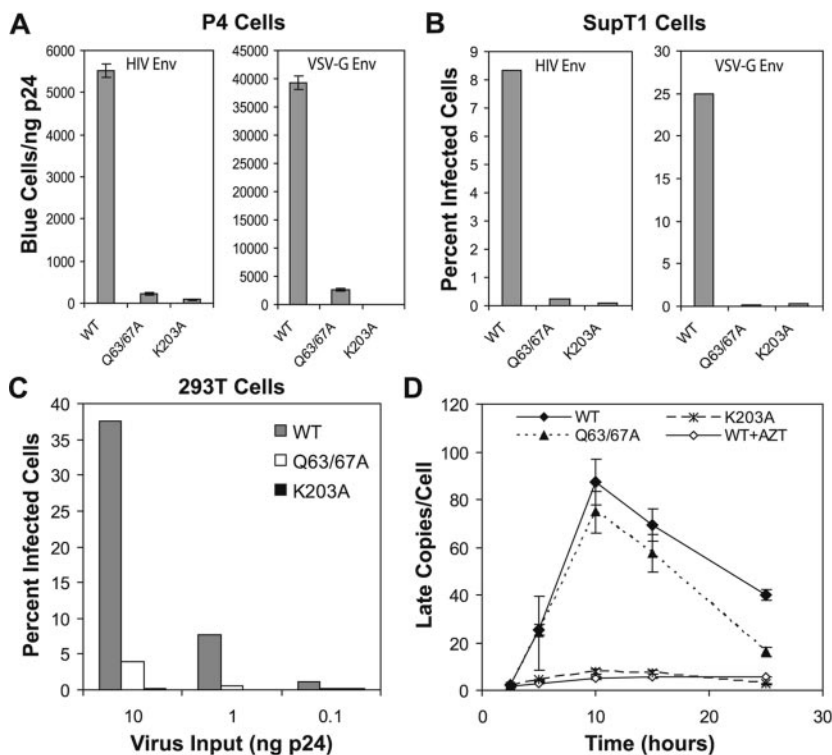


FIG. 3. The Q63/67A infectivity impairment is not rescued by VSV-G pseudotyping. Nonpseudotyped or VSV-G-pseudotyped viruses were used to infect P4 (A), SupT1 (B), or 293T (C) cells in single-cycle infectivity assays. Virus inocula were normalized by p24 ELISA. P4 cells were stained with X-Gal, and the infectivity was calculated as the number of blue cells per ng of p24. Shown are the mean values for triplicate infections, with error bars representing one standard deviation. Infection of 293T and SupT1 cells was quantified by flow cytometry following intracellular staining for HIV-1 Gag protein. For SupT1 cells (B), 100 ng p24 and 10 ng p24 of nonpseudotyped and VSV-G-pseudotyped viruses, respectively, were used for inoculations. WT, wild type. At various times postinfection the DNA from P4 target cells was isolated and HIV-1 late-product DNA quantified by real-time PCR (D) as previously described for Fig. 2. Results are representative of two independent experiments.

termini, thereby leading to reduced end-to-end ligation. Because the 1-LTR circular DNA form arises from homologous recombination and is therefore less likely to be affected by defects in the LTR ends, we asked whether the Q63/67A mu-

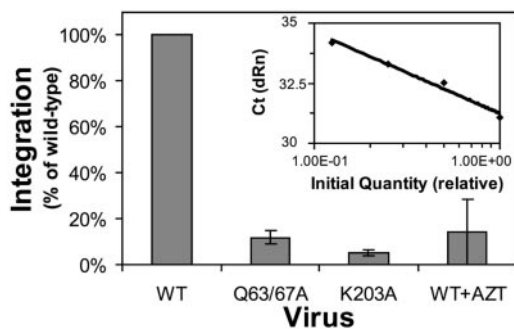


FIG. 4. The Q63/67A HIV-1 mutant is impaired for integration in vivo. P4 cells were inoculated with VSV-G-pseudotyped viruses. Cells were cultured for 14 days to allow the degradation of nonintegrated forms of viral DNA. A nested quantitative real-time PCR assay specific for integrated HIV-1 provirus was performed on DNA isolated from approximately  $5 \times 10^6$  infected cells. Twofold serial dilutions of DNA from cells infected with wild-type HIV-1 were assayed to generate a standard curve (inset) and the relative integration efficiencies of the mutants determined. Shown are the mean values for triplicate determinations, with error bars representing one standard deviation. Results are representative of two independent experiments.

tant particles were also impaired in synthesis of 1-LTR circles. For this purpose, DNA restriction fragments specifically released from 1-LTR circles were detected by Southern blotting (Fig. 5B). At 6 h postinfection, a strong band corresponding to linear HIV-1 cDNA was detected for both the control virus and the Q63/67A mutant. Cells inoculated with the control virus in the presence of AZT contained decreased levels of all DNA forms, demonstrating that they arose from reverse transcription (data not shown). By 24 h postinfection, a 2.8-kb band corresponding to the 1-LTR form of viral DNA was detected only in cells inoculated with the control pseudotyped virus. At 24 h, the levels of the linear form had decreased. These kinetics are consistent with previous studies demonstrating decay of the linear form of the viral DNA during this time frame (11, 47). By contrast to the control virus, the 1-LTR band produced by the Q63/67A virus was reduced in intensity. Quantification of the relative signals of the 1-LTR and linear HIV-1 DNA forms revealed a fourfold specific reduction in 1-LTR circle synthesis by the Q63/67A virus relative to the infectious control virions (Fig. 5C). However, this difference is likely an underestimate due to the significant degree of background present in the sample lanes. Collectively, the reduced quantities of 1-LTR and 2-LTR circular DNA forms in cells inoculated with the Q63/67A mutant particles indicate that the mutant PIC is impaired in its ability to access the nucleus.

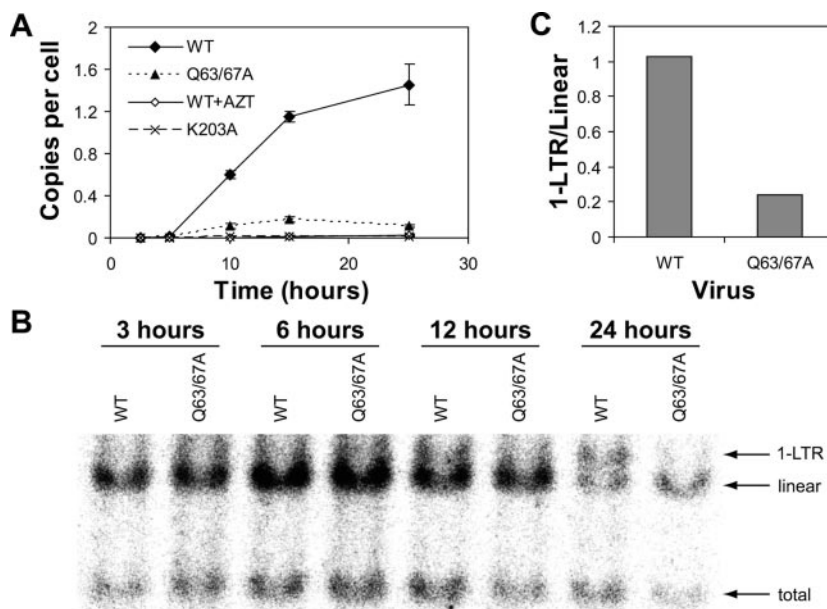


FIG. 5. Q63/67A mutant particles are impaired for nuclear entry. DNA extracted from SupT1 cells infected at low multiplicity of infection (MOI) (~1) (A) or high MOI (~15) (B) with wild-type (WT) and mutant viruses was subjected to real-time PCR detecting 2-LTR junction sequences (A) or analyzed by Southern blotting (B). Serial dilutions of plasmid DNA containing 2-LTR junctions were used to generate a standard curve, and the levels of 2-LTR circles in experimental samples were determined by interpolation from the curve. Infections were performed in duplicate, with duplicate quantitation of each sample (A). Values shown are the means of four determinations (duplicate measurements from two parallel samples), with error bars representing one standard deviation. Southern blots were probed with a <sup>32</sup>P-labeled probe detecting 1-LTR circles, linear proviral DNA, and total products (B) and detected on a Fujifilm FLA-2000 phosphorimager. Quantification of 1-LTR and linear product band signals was performed with ImageGauge software, and the ratios were calculated (C). Results are representative of three independent experiments.

**Q63/67A mutant PICs are impaired for integration in vitro.**

The reduction in circular DNA indicated that Q63/67A is specifically impaired at a step prior to nuclear import. If this were the only defect associated with the mutant particles, PICs recovered from cells inoculated with the mutant virions should be competent for integration into a target DNA molecule in vitro. To test this hypothesis, we extracted PICs from acutely infected cells and assayed their ability to integrate in vitro. Most previous studies of HIV-1 PICs have employed cells infected at high multiplicities by coculture of uninfected and chronically infected cells. To enhance recovery of PICs using infection with cell-free virus, VSV-G-pseudotyped control and CA mutant viruses were used to infect SupT1 target cells. At 8 h postinfection, cytoplasmic extracts were prepared by permeabilizing cells with a low concentration of a nonionic detergent. To assay the integration activity of the extracted PICs, samples containing similar quantities of full-length viral DNA were incubated with  $\phi$ X174 target DNA to allow integration. Integration products were quantified using a novel real-time PCR-based assay we developed. Reaction mixtures contained a TaqMan probe and a unique primer recognizing the 3' LTR, together with six individual primers complementary to the one strand of the  $\phi$ X174 target DNA. The sequences of the six target primers were chosen such that they were regularly spaced around the circular phage DNA molecule. This combination of primers results in amplification of only integrated DNA products, which are detected by cleavage of the TaqMan probe resulting from elongation from a  $\phi$ X174 primer into HIV-1 LTR sequences. Using this approach, we detected in-

tegration of wild-type HIV-1 DNA into target DNA (Fig. 6A). Reactions were linear with dilution of integration products (data not shown); furthermore, the signal was dependent on the quantity of PICs added to the integration reaction (Fig. 6A, inset graph). Importantly, we observed no signal for integration reactions that lacked target DNA, or reactions in which a specific integrase inhibitor (C5) was added (Fig. 6A). When PICs from Q63/67A-infected cells were used in this assay, we observed an approximately sevenfold reduction in integration activity compared to wild-type virus (Fig. 6A), despite the presence of similar quantities of late reverse transcripts in these samples (Fig. 6B). We conclude that, in addition to their impaired ability to enter the nucleus, the Q63/67A mutant PICs are also impaired for integration.

**Biochemical analysis of wild-type and Q63/67A PICs.** The lack of integration activity observed using Q63/67A PICs in vitro suggested that the mutant complexes might differ biochemically from wild-type PICs. To test this hypothesis, we analyzed the protein compositions of wild-type and mutant PICs following partial purification by velocity gradient sedimentation. SupT1 cells were infected with VSV-G-pseudotyped wild-type and Q63/67A viruses at high multiplicity (~15 infectious units per cell for wild type). Cytoplasmic extracts from infected cells were isolated at 8 h postinfection and subjected to velocity gradient ultracentrifugation over 10 to 50% linear sucrose gradients, and viral cDNA was quantified in the gradient fractions by real-time PCR. For both wild-type and Q63/67A mutant viruses, viral DNA (late reverse transcripts) was detected primarily in fraction 14, near the bottom of the gra-

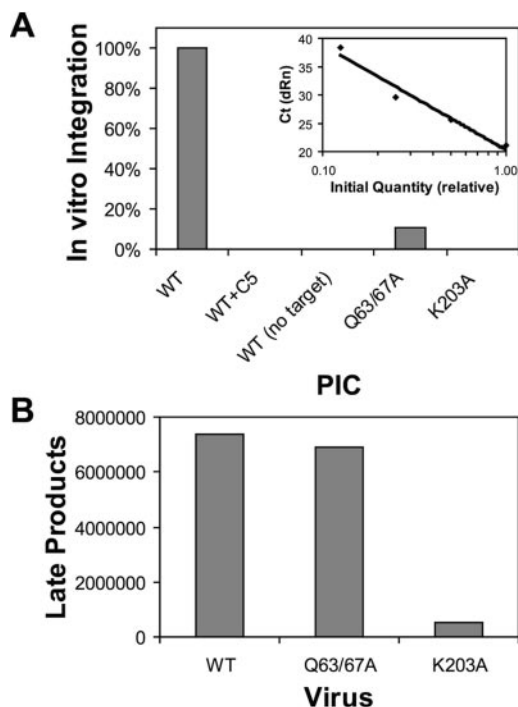


FIG. 6. Q63/67A mutant PICs are impaired for integration in vitro. Cytoplasmic extracts containing similar quantities of viral DNA were incubated in the presence or absence of 1  $\mu$ g of  $\phi$ X174 DNA for 45 min at 37°C. DNA was subsequently isolated and subjected to real-time PCR to detect integrated products (A) or late products of reverse transcription (B). As a control, wild-type (WT) HIV-1 infection was also performed in cultures containing the integrase inhibitor compound 5 (C5; 1  $\mu$ M). A standard curve corresponding to dilutions of an integration reaction is shown in the inset to panel A. Results are representative of three independent experiments.

dent (Fig. 7A). These late products are most likely present as part of a nucleoprotein complex, as they cosedimented with viral proteins (Fig. 7C and D), and treatment of the cell lysates with proteinase K prior to centrifugation resulted in a shift of the viral DNA to the upper fractions of the gradient (data not shown). Immunoblot analysis of the proteins in the gradient fractions further revealed that the viral DNA cosedimented with a small fraction of the total MA and IN proteins and that the Q63/67A complexes contained levels of MA and IN similar to wild-type PICs (Fig. 7C). In addition, comparable levels of exogenous reverse transcriptase activity were found for wild-type and mutant PIC-containing fractions (Fig. 7B), suggesting that the nuclear import and integration impairments for Q63/67A are not due to the loss of MA, IN, or RT from the PIC. By contrast, when gradients were analyzed for CA content by p24 ELISA, we detected a higher concentration of CA that cosedimented with Q63/67A PICs (Fig. 7D). The levels of PIC-associated CA were approximately sevenfold higher for the mutant versus wild type when normalized by MA content (Fig. 7E). Since the elevated level of CA is the sole biochemical defect we have detected in the mutant PICs, this suggests that association of the mutant CA with the PIC may inhibit its ability to enter the nucleus and mediate integration.

## DISCUSSION

In this study, we identified the replication defect for the Q63/67A HIV-1 CA mutant. The mutant particles undergo efficient fusion and reverse transcription yet are impaired for nuclear entry and integration in target cells. PICs formed by the Q63/67A mutant contain elevated levels of CA, suggesting that the mutant cores failed to completely uncoat. The mutant PICs were markedly impaired for integration in vitro, further suggesting that HIV-1 integration may depend on proper uncoating. We favor a model in which the incomplete dissociation of CA prevents the mutant PIC from gaining access to the nucleus. However, it is also possible that the failure of the mutant PICs to enter the nucleus is due to active sequestration in the cytoplasm or another intracellular compartment.

Upon entry into the cytosol of target cells, the capsid of HIV-1 disassociates from the viral RNP in a process of uncoating. HIV-1 uncoating has generally been assumed to occur rapidly and spontaneously. This assumption is based largely on negative data, including the absence of visible conical cores in electron micrographs of acutely infected cells (27) and the paucity of CA present in purified HIV-1 PICs (19, 36). Other studies have failed to detect CA in association with cytoplasmic reverse transcription complexes (RTCs) recovered from cells soon after inoculation (21, 37). However, the interaction of CA with the RTC could be relatively weak and could have been disrupted during RTC isolation. Recent work from our laboratory and others has suggested that uncoating is a regulated process. First, we identified CA mutants which exhibited a reduction in capsid stability relative to wild-type HIV-1; these were poorly infectious (25). These mutants, along with hyperstable cores, were impaired for reverse transcription in target cells, indicating that HIV-1 reverse transcription is dependent on association of CA with the viral core. Second, immunofluorescence imaging of intracellular HIV-1 particles revealed that HIV-1 reverse transcription complexes contained CA, suggesting that a fraction of the CA remains associated with the core during reverse transcription (35). Third, we have shown that the ability of HIV-1 to saturate host restriction in owl monkey cells requires HIV-1 particles with stable capsids (24). HIV-1 particles containing unstable cores were impaired in their ability to enhance infection by wild-type HIV-1 reporter virus in *trans*, indicating that the cytoplasmic restriction factor recognizes CA in the context of an intact core and that CA is likely associated with the core in the cytoplasm.

While the bulk of the current evidence indicates that some CA remains associated with the RTC, biochemical studies have detected little to no CA in association with purified PICs (19, 21, 36). The apparent lack of CA within the PIC suggests that complete dissociation of CA may be necessary for the formation of an active PIC. Consistent with this idea, we have found that the Q63/67A mutant exhibits an intermediate core yield (~50% of wild type) (25), suggesting that RTCs formed by this mutant may contain at least a portion of the normal level of CA. Since the Q63/67A mutant is competent for synthesis of both early and late reverse transcription products (Fig. 2), it appears that a sufficient quantity of CA associates with the mutant viral nucleoprotein complex to support HIV-1 reverse transcription.

Why do the Q63/67A mutant PICs fail to integrate in vitro? This impairment does not appear to result from a deficiency of

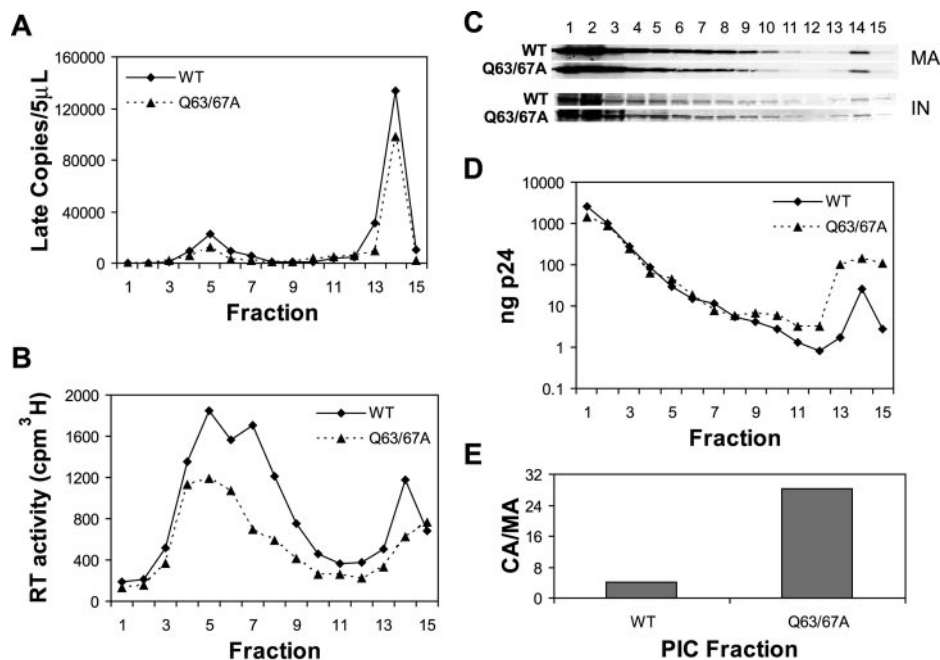


FIG. 7. Biochemical analysis of wild-type (WT) and Q63/67A mutant PICs. Cytoplasmic extracts from HIV-1-inoculated cells were fractionated by velocity sedimentation on 10 to 50% linear sucrose gradients. Fractions were collected from the top of the gradients and were analyzed for HIV-1 late-product DNA by quantitative PCR (A), reverse transcriptase activity (B), MA and IN by immunoblotting (C), and CA by ELISA (D). (E) The ratio of CA to MA was determined by dividing the CA concentration (D) in fraction 14 by the corresponding MA pixel intensity (C; quantified directly with a Li-Cor Odyssey), corresponding to the peak of viral DNA. Results are representative of two independent experiments.

IN, MA, or RT association with the PICs (Fig. 7C). One trivial possibility is that the mutant CA fails to adequately protect the viral DNA from nuclease digestion in the cytoplasm. A more detailed analysis of the HIV-1 DNA present in the mutant PICs may resolve this issue. It is also possible that the association of the mutant CA with the PICs inhibits integration activity by sterically interfering with the viral DNA ends or directly inhibiting IN activity. In this case, we predict that addition of Q63/67A mutant CA protein may inhibit integration of wild-type PICs *in vitro*. This hypothesis remains to be tested.

Collectively, our results are consistent with a model in which the uncoating of the HIV-1 capsid occurs through a progressive release of CA during the early steps of infection leading up to nuclear import of the PIC. Based on our previous finding that hyperstable mutants are impaired for reverse transcription (25), it is likely that partial capsid disassembly is required for initiation and completion of reverse transcription. Furthermore, we have consistently observed that loss of capsid protein from the internal RNP occurs through a biphasic disassembly process (23, 25). The majority of CA disassociates from the RNP during an initial phase of uncoating, followed by a slower secondary stage of capsid protein disassembly. The presence of elevated levels of CA in the Q63A/Q67A mutant PICs and their failure to enter the nucleus and integrate *in vitro* suggest that completion of uncoating must occur to render the PIC competent for the subsequent steps of nuclear import and integration.

Recently, additional evidence for a link between retroviral uncoating and nuclear entry has been reported. MLV, unlike HIV-1, is unable to infect nondividing cells. MLV also differs from HIV in its uncoating program; the PIC of MLV remains

coated with CA even at late times postinfection (22). A chimeric HIV-1 encoding the MA and CA regions of MLV was found to be specifically impaired in the infection of nondividing cells (44). This defect was determined to be at nuclear import, as determined by the lack of 2-LTR circles in nondividing cells. The authors suggested that stable association of the MLV CA with the viral PIC inhibits nuclear import by masking karyophilic signals within the PIC or structural hindrance of the particle. Thus, the nuclear import signal may come from an associated cellular protein, as suggested by recent reports that the cellular protein LEDGF/p75 targets the PIC to the nucleus through its interaction with IN (31, 33). However, the ability of HIV-1 to infect nondividing cells does not appear to depend on a special property of its IN protein (45). Further studies will be required to definitively determine whether the ability of lentiviruses to infect nondividing cells is due to their specific mechanism of uncoating.

#### ACKNOWLEDGMENTS

We thank Paul Spearman, Mark Denison, Gene Oltz, Todd Graham, and members of the Aiken laboratory for helpful suggestions. We also thank Derya Unutmaz for assistance with flow cytometry and Rick Bushman for the 2-LTR standard plasmid. The integrase inhibitor L-839616 (compound 5) was provided by Merck Research Laboratories. The following reagents were obtained from the NIH AIDS Research and Reference Reagent Program, Division of AIDS, NIAID, NIH: hybridoma 183-H12-5C (anti-HIV-1 CA) from Bruce Chesebro, rabbit antiserum to HIV-1 IN from Duane P. Grandgenett, and rabbit antiserum to HIV-1 MA from Paul Spearman.

This work was supported by grant AI050423 from the National Institutes of Health.

## REFERENCES

1. **Aiken, C.** 1997. Pseudotyping human immunodeficiency virus type 1 (HIV-1) by the glycoprotein of vesicular stomatitis virus targets HIV-1 entry to an endocytic pathway and suppresses both the requirement for Nef and the sensitivity to cyclosporin A. *J. Virol.* **71**:5871–5877.
2. **Ao, Z., X. Yao, and E. A. Cohen.** 2004. Assessment of the role of the central DNA flap in human immunodeficiency virus type 1 replication by using a single-cycle replication system. *J. Virol.* **78**:3170–3177.
3. **Bartz, S. R., M. E. Rogel, and M. Emerman.** 1996. Human immunodeficiency virus type 1 cell cycle control: Vpr is cytostatic and mediates G<sub>2</sub> accumulation by a mechanism which differs from DNA damage checkpoint control. *J. Virol.* **70**:2324–2331.
4. **Bouyac-Bertoia, M., J. D. Dvorin, R. A. Fouchier, Y. Jenkins, B. E. Meyer, L. I. Wu, M. Emerman, and M. H. Malim.** 2001. HIV-1 infection requires a functional integrase NLS. *Mol. Cell* **7**:1025–1035.
5. **Briggs, J. A., T. Wilk, R. Welker, H. G. Krausslich, and S. D. Fuller.** 2003. Structural organization of authentic, mature HIV-1 virions and cores. *EMBO J.* **22**:1707–1715.
6. **Brussel, A., and P. Sonigo.** 2003. Analysis of early human immunodeficiency virus type 1 DNA synthesis by use of a new sensitive assay for quantifying integrated provirus. *J. Virol.* **77**:10119–10124.
7. **Bukrinsky, M. I., S. Haggerty, M. P. Dempsey, N. Sharova, A. Adzhubel, L. Spitz, P. Lewis, D. Goldfarb, M. Emerman, and M. Stevenson.** 1993. A nuclear localization signal within HIV-1 matrix protein that governs infection of non-dividing cells. *Nature* **365**:666–669.
8. **Bukrinsky, M. I., N. Sharova, M. P. Dempsey, T. L. Stanwick, A. G. Bukrinskaya, S. Haggerty, and M. Stevenson.** 1992. Active nuclear import of human immunodeficiency virus type 1 preintegration complexes. *Proc. Natl. Acad. Sci. USA* **89**:6580–6584.
9. **Bukrinsky, M. I., N. Sharova, T. L. McDonald, T. Pushkarskaya, W. G. Tarpley, and M. Stevenson.** 1993. Association of integrase, matrix, and reverse transcriptase antigens of human immunodeficiency virus type 1 with viral nucleic acids following acute infection. *Proc. Natl. Acad. Sci. USA* **90**:6125–6129.
10. **Butler, S. L., M. S. Hansen, and F. D. Bushman.** 2001. A quantitative assay for HIV DNA integration in vivo. *Nat. Med.* **7**:631–634.
11. **Butler, S. L., E. P. Johnson, and F. D. Bushman.** 2002. Human immunodeficiency virus cDNA metabolism: notable stability of two-long terminal repeat circles. *J. Virol.* **76**:3739–3747.
12. **Cavrois, M., C. De Noronha, and W. C. Greene.** 2002. A sensitive and specific enzyme-based assay detecting HIV-1 virion fusion in primary T lymphocytes. *Nat. Biotechnol.* **20**:1151–1154.
13. **Charneau, P., M. Alizon, and F. Clavel.** 1992. A second origin of DNA plus-strand synthesis is required for optimal human immunodeficiency virus replication. *J. Virol.* **66**:2814–2820.
14. **Chazal, N., G. Singer, C. Aiken, M. L. Hammarskjold, and D. Rekosh.** 2001. Human immunodeficiency virus type 1 particles pseudotyped with envelope proteins that fuse at low pH no longer require Nef for optimal infectivity. *J. Virol.* **75**:4014–4018.
15. **Chen, C., and H. Okayama.** 1987. High-efficiency transformation of mammalian cells by plasmid DNA. *Mol. Cell. Biol.* **7**:2745–2752.
16. **Chen, H., S. Q. Wei, and A. Engelman.** 1999. Multiple integrase functions are required to form the native structure of the human immunodeficiency virus type 1 intasome. *J. Biol. Chem.* **274**:17358–17364.
17. **Dvorin, J. D., P. Bell, G. G. Maul, M. Yamashita, M. Emerman, and M. H. Malim.** 2002. Reassessment of the roles of integrase and the central DNA flap in human immunodeficiency virus type 1 nuclear import. *J. Virol.* **76**:12087–12096.
18. **Farnet, C. M., and F. D. Bushman.** 1997. HIV-1 cDNA integration: requirement of HMGI(Y) protein for function of preintegration complexes in vitro. *Cell* **88**:483–492.
19. **Farnet, C. M., and W. A. Haseltine.** 1991. Determination of viral proteins present in the human immunodeficiency virus type 1 preintegration complex. *J. Virol.* **65**:1910–1915.
20. **Farnet, C. M., and W. A. Haseltine.** 1990. Integration of human immunodeficiency virus type 1 DNA in vitro. *Proc. Natl. Acad. Sci. USA* **87**:4164–4168.
21. **Fassati, A., and S. P. Goff.** 2001. Characterization of intracellular reverse transcription complexes of human immunodeficiency virus type 1. *J. Virol.* **75**:3626–3635.
22. **Fassati, A., and S. P. Goff.** 1999. Characterization of intracellular reverse transcription complexes of Moloney murine leukemia virus. *J. Virol.* **73**:8919–8925.
23. **Forshey, B. M., and C. Aiken.** 2003. Disassembly of human immunodeficiency virus type 1 cores in vitro reveals association of Nef with the subviral ribonucleoprotein complex. *J. Virol.* **77**:4409–4414.
24. **Forshey, B. M., J. Shi, and C. Aiken.** 2005. Structural requirements for recognition of the human immunodeficiency virus type 1 core during host restriction in owl monkey cells. *J. Virol.* **79**:869–875.
25. **Forshey, B. M., U. von Schwedler, W. I. Sundquist, and C. Aiken.** 2002. Formation of a human immunodeficiency virus type 1 core of optimal stability is crucial for viral replication. *J. Virol.* **76**:5667–5677.
26. **Freed, E. O., and M. A. Martin.** 1995. Virion incorporation of envelope glycoproteins with long but not short cytoplasmic tails is blocked by specific, single amino acid substitutions in the human immunodeficiency virus type 1 matrix. *J. Virol.* **69**:1984–1989.
27. **Grewe, C., A. Beck, and H. R. Gelderblom.** 1990. HIV: early virus-cell interactions. *J. Acquir. Immune Defic. Syndr.* **3**:965–974.
28. **Khiytani, D. K., and N. J. Dimmock.** 2002. Characterization of a human immunodeficiency virus type 1 pre-integration complex in which the majority of the cDNA is resistant to DNase I digestion. *J. Gen. Virol.* **83**:2523–2532.
29. **Limon, A., N. Nakajima, R. Lu, H. Z. Ghory, and A. Engelman.** 2002. Wild-type levels of nuclear localization and human immunodeficiency virus type 1 replication in the absence of the central DNA flap. *J. Virol.* **76**:12078–12086.
30. **Lin, C. W., and A. Engelman.** 2003. The barrier-to-autointegration factor is a component of functional human immunodeficiency virus type 1 preintegration complexes. *J. Virol.* **77**:5030–5036.
31. **Llano, M., M. Vanegas, O. Fregoso, D. Saenz, S. Chung, M. Peretz, and E. M. Poeschla.** 2004. LEDGF/p75 determines cellular trafficking of diverse lentiviral but not murine oncoretroviral integrase proteins and is a component of functional lentiviral preintegration complexes. *J. Virol.* **78**:9524–9537.
32. **Luo, T., J. L. Douglas, R. L. Livingston, and J. V. Garcia.** 1998. Infectivity enhancement by HIV-1 Nef is dependent on the pathway of virus entry: implications for HIV-based gene transfer systems. *Virology* **241**:224–233.
33. **Maertens, G., P. Cherepanov, W. Plumeyers, K. Busschots, E. De Clercq, Z. Debyser, and Y. Engelborghs.** 2003. LEDGF/p75 is essential for nuclear and chromosomal targeting of HIV-1 integrase in human cells. *J. Biol. Chem.* **278**:33528–33539.
34. **Mammano, F., E. Kondo, J. Sodroski, A. Bukovsky, and H. G. Gottlinger.** 1995. Rescue of human immunodeficiency virus type 1 matrix protein mutants by envelope glycoproteins with short cytoplasmic domains. *J. Virol.* **69**:3824–3830.
35. **McDonald, D., M. A. Vodicka, G. Lucero, T. M. Svitkina, G. G. Borisy, M. Emerman, and T. J. Hope.** 2002. Visualization of the intracellular behavior of HIV in living cells. *J. Cell Biol.* **159**:441–452.
36. **Miller, M. D., C. M. Farnet, and F. D. Bushman.** 1997. Human immunodeficiency virus type 1 preintegration complexes: studies of organization and composition. *J. Virol.* **71**:5382–5390.
37. **Nermut, M. V., and A. Fassati.** 2003. Structural analyses of purified human immunodeficiency virus type 1 intracellular reverse transcription complexes. *J. Virol.* **77**:8196–8206.
38. **Popov, S., M. Rexach, G. Zybarth, M. A. Lee, L. Ratner, C. M. Lane, M. S. Moore, G. Blobel, and M. Bukrinsky.** 1998. Viral protein R regulates nuclear import of the HIV-1 pre-integration complex. *EMBO J.* **17**:909–917.
39. **Stevenson, M.** 2002. Molecular biology of lentivirus-mediated gene transfer. *Curr. Top. Microbiol. Immunol.* **261**:1–30.
40. **von Schwedler, U. K., K. M. Stray, J. E. Garrus, and W. I. Sundquist.** 2003. Functional surfaces of the human immunodeficiency virus type 1 capsid protein. *J. Virol.* **77**:5439–5450.
41. **Wai, J. S., M. S. Egbertson, L. S. Payne, T. E. Fisher, M. W. Embrey, L. O. Tran, J. Y. Melamed, H. M. Langford, J. P. Guare, Jr., L. Zhuang, V. E. Grey, J. P. Vacca, M. K. Holloway, A. M. Naylor-Olsen, D. J. Hazuda, P. J. Felock, A. L. Wolfe, K. A. Stillmock, W. A. Schleif, L. J. Gabryelski, and S. D. Young.** 2000. 4-Aryl-2,4-dioxobutanoic acid inhibitors of HIV-1 integrase and viral replication in cells. *J. Med. Chem.* **43**:4923–4926.
42. **Wehrly, K., and B. Chesebro.** 1997. p24 antigen capture assay for quantification of human immunodeficiency virus using readily available inexpensive reagents. *Methods* **12**:288–293.
43. **Wyma, D. J., J. Jiang, J. Shi, J. Zhou, J. E. Lineberger, M. D. Miller, and C. Aiken.** 2004. Coupling of human immunodeficiency virus type 1 fusion to virion maturation: a novel role of the gp41 cytoplasmic tail. *J. Virol.* **78**:3429–3435.
44. **Yamashita, M., and M. Emerman.** 2004. Capsid is a dominant determinant of retrovirus infectivity in nondividing cells. *J. Virol.* **78**:5670–5678.
45. **Yamashita, M., and M. Emerman.** 2005. The cell cycle independence of HIV infections is not determined by known karyophilic viral elements. *PLoS Pathog.* **1**:e18.
46. **Yee, J. K., T. Friedmann, and J. C. Burns.** 1994. Generation of high-titer pseudotyped retroviral vectors with very broad host range. *Methods Cell Biol.* **43**(Pt. A):99–112.
47. **Zennou, V., C. Petit, D. Guetard, U. Nerhass, L. Montagnier, and P. Charneau.** 2000. HIV-1 genome nuclear import is mediated by a central DNA flap. *Cell* **101**:173–185.
48. **Zhou, J., and C. Aiken.** 2001. Nef enhances human immunodeficiency virus type 1 infectivity resulting from intervirion fusion: evidence supporting a role for Nef at the virion envelope. *J. Virol.* **75**:5851–5859.